

Long Baseline Interferometric Observations of Cepheids.

Benjamin F. Lane

Department of Geological & Planetary Sciences, MS 150-21, California Institute of Technology, Pasadena CA 91125, U.S.A.

`ben@gps.caltech.edu`

Michelle J. Creech-Eakman

Caltech/JPL Postdoctoral Scholar, Jet Propulsion Laboratory, California Institute of Technology, 4800 Oak Grove Drive, Pasadena, CA 91109, U.S.A.

`mce@huey.jpl.nasa.gov`

and

Tyler E. Nordgren

University of Redlands, Department of Physics, 1200 E Colton Ave, Redlands, California, U.S.A.

`Tyler_Nordgren@redlands.edu`

ABSTRACT

We present observations of the galactic cepheids η Aql and ζ Gem. Our observations are able to resolve the diameter changes associated with pulsation. This allows us to determine the distance to the Cepheids independent of photometric observations. We determine a distance to η Aql of 320 ± 32 pc, and a distance to ζ Gem of 362 ± 38 pc. These observations allow us to calibrate surface brightness relations for use in extra-galactic distance determination. They also provide a measurement of the mean diameter of these Cepheids, which is useful in constructing structural models of this class of star.

Subject headings: Cepheids— stars:fundamental parameters—stars:individual (η Aquilae, ζ Geminorum)

1. Introduction

The class of pulsating stars known as Cepheids is a cornerstone in determining the distances to nearby galaxies. This is because Cepheids exhibit a well-behaved period-luminosity relation which can be locally calibrated (Jacoby et al. 1992). In addition, these stars are massive and thus intrinsically very luminous, making it possible to observe Cepheids located in very distant galaxies (Tanvir 1999; Feast 1999). Because of the usefulness and fundamental importance of Cepheids, it is important to calibrate their period-luminosity relation. This has been done using a variety of methods, including parallax (ESA 1997; Feast & Catchpole 1997), Baade-Wesselink methods (Wesselink 1946; Bersier et al. 1997) and surface brightness (Laney & Stobie 1995; Fouque & Gieren 1997; Ripepi et al. 1997). The period-luminosity relations used currently have uncertainties on the order of 0.09 mag (Feast 1999), which in turn make up a significant portion of the systematic uncertainty in estimates to the Large Magellanic Cloud.

Using long-baseline stellar interferometry it is possible to resolve the diameter changes undergone by a nearby Cepheid during a pulsational cycle. When such diameter measurements are combined with radial velocity measurements of the stellar photosphere, it is possible to determine the size of and distance to the Cepheid. Such a direct measurement is independent of photometric observations and their associated uncertainties.

The Palomar Testbed Interferometer (PTI) is located on Palomar Mountain near San Diego, CA (Colavita et al. 1999). It combines starlight from two 40-cm apertures to measure the amplitude (a.k.a. visibility) of the resulting interference fringes. There are two available baselines, one 110-m baseline oriented roughly North-South (hereafter N-S), and one 85-m baseline oriented roughly North-Southwest (called N-W). In a previous paper (Lane et al. 2000) we presented observations using PTI of the Cepheid ζ Gem. Here we report on additional interferometric observations of ζ Gem, as well as a second Galactic Cepheid, η Aql. These observations allow us to determine the distances to these Cepheids with the aim of reducing the uncertainty in currently used period-luminosity relations for Cepheids.

2. Observations

We observed the nearby galactic cepheids η Aql and ζ Gem on 22 nights between 2001 March 13 and 2001 July 26. The observing procedure followed standard PTI practice (Boden et al. 1998; Colavita et al. 1999). For the observations of η Aql the N-W baseline was used, while observations of ζ Gem used the N-S baseline. Each nightly observation consisted of approximately ten 130-second integrations during which the fringe visibility was averaged.

The measurements were done in the $1.52 - 1.74 \mu\text{m}$ (effective central wavelength $1.65 \mu\text{m}$) wavelength region, similar to the astronomical H band. Observations of calibration sources were rapidly (within less than ~ 10 minutes) interleaved with the Cepheid observations, and after each 130-second integration the apertures were pointed to dark sky and a 30-second measurement of the background light level was made.

The calibrators were selected to be located no more than 16 degrees from the primary target on the sky and to have similar H -band magnitudes. In choosing calibration sources we avoided known binary or highly variable stars. The calibrators used are listed in Table 2. In this paper we make use of previously published observations of the Cepheid ζ Gem (Lane et al. 2000). However, in order to improve on the previously published results we carried out additional observations of this source on 2001 March 13–15. We also observed additional unresolved calibrators in order to reduce the level of systematic uncertainty. The original data have been jointly re-reduced using the improved calibrator diameters and uncertainties. However, note that the primary calibrator diameter has not changed from the value used in Lane et al. (2000).

3. Analysis & Results

3.1. Fringe Visibilities & Limb Darkening

PTI uses either a 10 or 20 ms sample rate. Each such sample provides a measure of the instantaneous fringe visibility and phase. While the phase value is converted to distance and fed back to the active delay line to provide active fringe tracking, the measured fringe visibility is averaged over the entire 130-second integration. The statistical uncertainty in each measurement is estimated by breaking the 130 second integration into five equal-time segments and measuring the standard deviation about the mean value.

The theoretical relation between source brightness distribution and fringe visibility is given by the van Cittert-Zernike theorem. For a uniform intensity disk model the normalized fringe visibility (squared) can be related to the apparent angular diameter as

$$V^2 = \left(\frac{2 J_1(\pi B \theta_{UD} / \lambda_0)}{\pi B \theta_{UD} / \lambda_0} \right)^2 \quad (1)$$

where J_1 is the first-order Bessel function, B is the projected aperture separation, θ_{UD} is the apparent angular diameter of the star in the uniform-disk model, and λ_0 is the center-band wavelength of the observation. It follows that the fringe visibility of a point source measured by an ideal interferometer should be unity. For a more realistic model that includes limb

darkening one can derive a conversion factor between a uniform-disk diameter (θ_{UD}) and a limb-darkened disk diameter (θ_{LD}) given by (Welch 1994)

$$\theta_{UD} = \theta_{LD} \sqrt{1 - \frac{A}{3} - \frac{B}{6}} \quad (2)$$

where A and B are quadratic limb darkening coefficients, determined by the spectral type of the source (Claret et al. 1995). The limb darkening correction factors ($k = \theta_{UD}/\theta_{LD}$) used for the Cepheids are shown in Table 1 and for the calibrators in Table 2.

3.2. Visibility Calibration

The first step in calibrating visibilities measured by PTI is to correct for the effects of detector background and read-noise, the details of which are discussed in Colavita et al. (1999) and Colavita (1999). However, the visibilities thus produced are not yet final: due to a variety of effects, including systematic instrumental effects, intensity mismatches, and atmospheric turbulence, the fringe visibility of a source measured by PTI is lower than that predicted by Eq. 1. In practice the system response function (called the system visibility) is typically ~ 0.75 and furthermore is variable on 30 minute timescales. Hence the visibilities must be calibrated by observing sources of known diameter.

Determining the diameter of the calibration sources was a multi-step process in which we made use of both models and prior observations. For each Cepheid we designated a single, bright K giant as a primary calibrator, which was always observed in close conjunction with the target Cepheid (HD 189695 for η Aql, and HD 49968 for ζ Gem). We used model diameter estimates for the primary calibrators from previously published results based on spectro-photometry and modeling (Cohen et al. 1999).

In order to verify that the primary calibrators were stable and had angular diameters consistent with the Cohen et al. (1999) results, we observed them together with a number of secondary calibrators. These secondary calibrators were typically less resolved than the primary calibrators and hence less sensitive to uncertainties in their expected angular diameter. However, they were fainter than the primary calibrators, and tended to be located further away on the sky. For the secondary calibrators an apparent diameter was estimated using three methods: (1) we used available archival photometry to fit a black-body model by adjusting the apparent angular diameter, bolometric flux and effective temperature of the star in question so as to fit the photometry. (2) We repeated the above fit while constraining the effective temperature to the value expected based on the published spectral type. (3) We estimated the angular diameter of the star based on expected physical size (derived from

spectral type) and distance (determined by Hipparcos). We adopted the weighted (by the uncertainty in each determination) mean of the results from the above methods as the final model diameter for the secondary calibrators, and the uncertainty in the model diameter was taken to be the deviation about the mean.

In addition to the model-based diameter estimates derived above we also used extensive interferometric visibility measurements for the primary and secondary calibrators; given that several of the calibrators were observed within a short enough period of time that the system visibility could be treated as constant, it was possible to find a set of assumed calibrator diameters that are maximally self-consistent, by comparing observed diameter ratios for which the system visibility drops out. To illustrate, let θ_i be an adjustable parameter, representing the diameter of star i . Let $\hat{\theta}_i$ and $\sigma_{\hat{\theta}_i}$ be the theoretical model diameter and uncertainty for star i derived above, and let \tilde{R}_{ij} and $\sigma_{\tilde{R}_{ij}}$ be the interferometrically observed diameter ratio and uncertainty of stars i and j . For notational simplicity, define R_{ij} as the ratio of θ_i and θ_j . Define the quantity

$$\chi^2 = \sum_i \left[\frac{\hat{\theta}_i - \theta_i}{\sigma_{\hat{\theta}_i}} \right]^2 + \sum_i \sum_{j < i} \left[\frac{\tilde{R}_{ij} - R_{ij}}{\sigma_{\tilde{R}_{ij}}} \right]^2 \quad (3)$$

By adjusting the set of θ_i to minimize χ^2 we produce a set of consistent calibrator diameters, taking into account both input model knowledge and observations. The resulting diameter values are listed in Table 2. Uncertainties were estimated using the procedure outlined in Press et al. (1986) assuming normally distributed errors.

We verified that the primary calibrators were stable as follows: using the secondary calibrators to calibrate all observations of the primary calibrators we fit a constant-diameter, single-star, uniform-disk model to the primary calibrators. In all cases the scatter about the single-star model was similar to expected system performance (Boden et al. 1998): for HD 189695, 21 points were fit, the average deviation in V^2 was 0.035 and the goodness-of-fit parameter of the line fit, χ^2 per degree of freedom (χ_{dof}^2 , not to be confused with Eq. 3 above), in the line fit was 0.46. For HD 49968, 82 points were fit, the average deviation was 0.038 and $\chi_{dof}^2 = 0.76$.

While analyzing the data it was noticed that during observations with the N–W baseline of relatively low declination sources, such as η Aql and its calibrators, the stability of the interferometer system visibility was strongly dependent on the hour angle of the source: for observations of η Aql obtained at positive hour angles the scatter in the system visibility increased by a factor of 2–3, while the mean value trended down by 20%/hr. There are two potential explanations for this effect: (1) for these observations the optical delay lines are close to their maximum range, which can exacerbate internal system misalignments and

Star Name	Alternate Name	Period (d)	Epoch JD	Limb Dark. Factor (k)
η Aql	HD 187929	7.176711	2443368.962	0.97 ± 0.01
ζ Gem	HD 52973	10.150079	2444932.736	0.96 ± 0.01

Table 1: Relevant parameters of the Cepheids. The limb darkening factor is defined as $k = \theta_{UD}/\theta_{LD}$.

Calibrator	Spectral Type	Diameter Used θ_{UD} (mas)	Limb Dark. Factor (k)	Used to calibrate	Cal. Type	Angular Sep. (deg)
HD 189695	K5 III	1.89 ± 0.07	0.943 ± 0.007	η Aql	Pri. Cal	7.8
HD 188310	G9.5 IIIb	1.57 ± 0.08	0.955 ± 0.007	η Aql	Sec. Cal	8.2
HD 181440	B9 III	0.44 ± 0.05	0.975 ± 0.007	η Aql	Sec. Cal	7.5
HD 49968	K5 III	1.78 ± 0.02	0.939 ± 0.006	ζ Gem	Pri. Cal	4.1
HD 48450	K4 III	1.94 ± 0.02	0.949 ± 0.007	ζ Gem	Sec. Cal	9.5
HD 39587	G0 V	1.09 ± 0.04	0.963 ± 0.006	ζ Gem	Sec. Cal	16
HD 52711	G4 V	0.55 ± 0.04	0.962 ± 0.006	ζ Gem	Sec. Cal	8.8

Table 2: Relevant parameters of the calibrators. The angular separation listed is the angular distance from the calibrator to the Cepheid it is used to calibrate.

lead to vignetting. (2) When observing low declination sources past transit, the siderostat orientation is such that surface damage near the edge of one of the siderostat mirrors causes vignetting. Thus it was decided to discard observations of η Aql taken at positive hour angles, corresponding to $\sim 20\%$ of the available data. We note that including the data does not significantly change the final results ($\sim 0.3\sigma$), it merely increases the scatter substantially (for the pulsation fit discussed below the goodness-of-fit parameter χ_{dof}^2 increased from 1.06 to 4.5).

3.3. Apparent Angular Diameter

Once the measured visibilities were calibrated we used all the available calibrated data from a given night to determine the apparent uniform-disk angular diameter of the target Cepheid on that particular night by fitting to a model given by Eq. 1. Results are given in Tables 3 and 4 and plotted in Fig. 1. Uncertainties were estimated based on the scatter about the best fit. It should be noted that although η Aql is known to have a companion (Bohm-Vitense & Proffitt 1985) it is sufficiently faint (average $\Delta m_H = 5.75$ mag) that it will have a negligible effect ($\Delta V^2 \sim 0.005$) on the fringe visibilities measured in the H band.

It is clear from Fig. 1 that the measured angular diameters are not constant with time. Fitting a constant-diameter model to the data produces a rather poor fit (see Table 5). However, we list the resulting mean angular diameters in order to facilitate comparison with previous interferometric results.

3.4. Distances & Radii

Determining the distance and radius of a Cepheid via the Baade-Wesselink method requires comparing the measured changes in angular diameter to the expansion of the Cepheid photosphere measured using radial velocity techniques. In order to determine the expansion of the Cepheid photospheres we fit a fifth-order Fourier series to previously published radial velocities. For η Aql we used data from Bersier (2002) as well as data published by Jacobsen & Wallerstein (1981, 1987), while for ζ Gem we used data from Bersier et al. (1994). Both sets of data were from measurements made at optical wavelengths. The measured radial velocities were converted to physical expansion rates using a projection factor (p-factor), which depends on the detailed atmospheric structure and limb darkening of the Cepheid as well as on the details of the equipment and software used in the measurement (Hindsley & Bell 1986; Albrow & Cottrell 1994). It is important to note that the p-factor is not expected

Epoch JD-2400000.5	Angular Diameter θ_{UD} (mas)	No. Scans
52065.420	1.654 ± 0.011	9
52066.414	1.654 ± 0.017	9
52067.405	1.694 ± 0.040	8
52075.383	1.740 ± 0.027	12
52076.384	1.799 ± 0.014	9
52077.372	1.822 ± 0.021	13
52089.350	1.715 ± 0.019	11
52090.354	1.798 ± 0.020	9
52091.346	1.764 ± 0.022	7
52095.360	1.567 ± 0.049	1
52099.337	1.800 ± 0.025	2
52101.329	1.632 ± 0.037	5
52103.293	1.656 ± 0.040	7
52105.300	1.798 ± 0.024	6
52106.283	1.816 ± 0.016	19
52107.302	1.809 ± 0.027	11
52108.308	1.702 ± 0.032	7
52116.276	1.611 ± 0.023	7

Table 3: The measured uniform-disk diameters of η Aql. The uncertainties are the statistical uncertainty from the scatter during a night, and do not include systematic uncertainty in the calibrator diameters; this adds an additional uncertainty of 0.07 mas in the aggregate mean diameter.

Epoch	Angular Diameter	No. Scans
JD-2400000.5	θ_{UD} (mas)	
51605.226	1.676 ± 0.015	15
51606.241	1.675 ± 0.047	3
51614.192	1.797 ± 0.060	7
51615.180	1.737 ± 0.031	10
51617.167	1.587 ± 0.028	10
51618.143	1.534 ± 0.008	11
51619.168	1.549 ± 0.018	15
51620.169	1.585 ± 0.028	15
51622.198	1.673 ± 0.046	6
51643.161	1.663 ± 0.012	9
51981.182	1.685 ± 0.014	23
51982.164	1.636 ± 0.020	16
51983.201	1.589 ± 0.021	15
51894.387	1.619 ± 0.019	13
51895.369	1.629 ± 0.014	12

Table 4: The measured uniform-disk diameters of ζ Gem. The uncertainties are the statistical uncertainty from the scatter during a night, and do not include systematic uncertainty in the calibrator diameters; this adds an additional uncertainty of 0.024 mas in the aggregate mean diameter.

to stay constant during a pulsational cycle. The exact phase dependence of the p-factor is beyond the scope of this paper. However, for η Aql and ζ Gem, the net effect of a variable p-factor can be approximated by using a 6% larger constant p-factor (Sabbey et al. 1995). Thus for both Cepheids we use an effective p-factor of 1.43 ± 0.06 , constant for all pulsational phases.

We convert the radial velocity Fourier series into a physical size change by integrating and multiplying by limb-darkening and p-factors. Although the limb-darkening does vary with changing T_{eff} during a pulsational cycle, the effect is small: for ζ Gem k varies from 0.960 to 0.967, i.e. less than the quoted uncertainty. The size change can in turn be converted into an angular size model with three free parameters: the mean physical radius, the distance to the star, and a phase shift. The latter is to account for possible period changes, inaccuracies in period or epoch, or phase lags due to level effects (where the optical and infrared photospheres are at different atmospheric depths; see below). We adjust the model phase, radius and distance to fit the observed angular diameters. Results of the fits for η Aql and ζ Gem are given in Table 5.

There are several sources of uncertainty in the above fits: in addition to the purely statistical uncertainty there are systematic uncertainties of comparable magnitude. The three primary sources of systematic uncertainty are: uncertainty in the calibrator diameters, uncertainty in the p-factor, and uncertainty in the limb darkening coefficients. The magnitude of each effect was estimated separately by re-fitting the model while varying by $\pm 1\sigma$ each relevant parameter separately. The total systematic uncertainty was calculated as

$$\sigma_{sys}^2 = \sigma_{cal}^2 + \sigma_{p-fac}^2 + \sigma_{limbdark}^2. \quad (4)$$

In order to explore the possibility of wavelength-dependent effects on the measured radial velocity, e.g. due to velocity gradients in the Cepheid atmospheres (“level effects”), we re-fit for the radius and distance of η Aql using a radial velocity curve based on radial velocity data obtained at wavelengths of 1.1 and $1.6\mu\text{m}$ by Sasselov & Lester (1990). Because of the limited number of observations available (e.g. only 3 H -band measurements of η Aql) we used the shape of the radial velocity curve derived from the fit to the optical data (i.e. by using the same Fourier coefficients); the IR data was only used to determine an overall amplitude of the velocity curve. For the IR points we used an effective p-factor of 1.41 ± 0.03 as recommended by D. Sasselov (private communication) and based on an analysis by Sabbey et al. (1995), taking into account both the use of a constant p-factor and the use of parabolic line fitting. The resulting best-fit parameters are very similar to those based on optical radial velocities (i.e. Table 5): $D = 333 \pm 30$ pc and $R = 64.2 \pm 6R_{\odot}$. A similar fit for ζ Gem gives $D = 359 \pm 37$ pc and $R = 62.2 \pm 5.7R_{\odot}$. Hence we conclude that the effects of wavelength dependence of the radial velocity are at present smaller than other sources of uncertainty.

Cepheid	Fit Type	Parameter	Best-Fit Results
			Value $\pm \sigma_{Tot}$ ($\sigma_{Stat.}/\sigma_{Sys.}$)
η Aql	Pulsation Fit	Distance (D)	320 ± 32 (24/21) pc
	No. Pts. = 18	Radius (R)	61.8 ± 7.6 (4.5/6.1) R_{\odot}
	$\chi_{dof}^2 = 1.06$	Phase (ϕ)	0.02 ± 0.011 ($0.011/5 \times 10^{-4}$) cycles
	Line Fit	θ_{UD}	1.734 ± 0.070 (0.018/0.068) mas
			$\chi_{dof}^2 = 13.4$
ζ Gem	Pulsation Fit	Distance (D)	362 ± 38 (35/15) pc
	No. Pts. = 15	Radius (R)	66.7 ± 7.2 (6.3/3.4) R_{\odot}
	$\chi_{dof}^2 = 1.82$	Phase (ϕ)	0.013 ± 0.016 ($0.016/3 \times 10^{-5}$) cycles
	Line Fit	θ_{UD}	1.613 ± 0.029 (0.017/0.024) mas
			$\chi_{dof}^2 = 14.6$

Table 5: Best-fit Cepheid parameters and their uncertainties, as well as mean apparent uniform-disk angular diameter (θ_{UD}) determined from fitting a line to all of the data. The uncertainties of the best-fit parameters are broken down into statistical ($\sigma_{Stat.}$) and systematic ($\sigma_{Sys.}$) uncertainties. The goodness-of-fit parameter is a weighted χ^2 divided by the number of degrees of freedom (χ_{dof}^2) in the fit. The χ_{dof}^2 of the fits are calculated from data that does not have the systematic (calibrator) uncertainty folded in since it applies equally to all points.

Cepheid	Reference	Radius R_{\odot}	Distance (pc)	Angular Diameter θ_{LD} (mas)
η Aql	this work	61.8 ± 7.6	320 ± 32	1.793 ± 0.070
	Nordgren et al. (2000)			1.69 ± 0.04
	Ripepi et al. (1997)	57 ± 3		
	ESA (1997)		360^{+174}_{-89}	
	Sasselov & Lester (1990)	62 ± 6		
	Fernley, Skillen, & Jameson (1989)	53 ± 5	275 ± 28	
	Moffett & Barnes (1987)	55 ± 4		
ζ Gem	this work	66.7 ± 7.2	362 ± 38	1.675 ± 0.029
	Lane et al. (2000)	62 ± 11	336 ± 44	1.62 ± 0.3
	Kervella et al. (2001)			$1.69^{+0.14}_{-0.16}$
	Nordgren et al. (2000)			1.55 ± 0.09
	ESA (1997)		358^{+147}_{-81}	
	Ripepi et al. (1997)	86 ± 4		
	Bersier et al. (1997)	89.5 ± 13	498 ± 84	
	Krockenberger, Sasselov, & Noyes (1997)	$69.1^{+5.5}_{-4.8}$		
	Sabbey et al. (1995)	64.4 ± 3.6		
Moffett & Barnes (1987)	65 ± 12			

Table 6: A comparison between the various available radius, distance and angular size determinations. The Nordgren et al. (2000) results are based on R band (740 nm) observations, while the Kervella et al. (2001) result is in the K band (2.2 μm).

The derived parameters (mean radius, distance and mean uniform-disk angular diameter) can be compared to previously published values, derived using a range of techniques (see Table 6), including parallax and a variety of surface brightness techniques. There are also several interferometric diameter measurements available in the literature, although to date no other interferometers have directly resolved Cepheid pulsations. Thus, directly measured angular diameters can only be compared in a phase-averaged sense.

3.5. Surface Brightness Relations

A wide variety of Cepheid surface brightness relations have been used by various authors (Barnes & Evans 1976; Laney & Stobie 1995; Fouque & Gieren 1997) to derive Cepheid distance scales. We define as surface brightness the quantity

$$F_i = 4.2207 - 0.1m_i - 0.5 \log(\theta_{LD}) \quad (5)$$

where F_i is the surface brightness in magnitudes in passband i , m_i is the apparent magnitude in that band, and θ_{LD} is the apparent angular diameter of the star. With the above relation and a good estimate of F_i one can determine the angular diameter based on photometry alone. Conversely, given measured angular diameters and multi-band photometry it is possible to calibrate F_i by finding a simple (e.g. linear) relation between F_i and a variety of color indices (e.g $V - K$). We define the following relations

$$F_{V,1} = a + b(V - K) \quad (6)$$

$$F_{V,2} = a + c(V - R) \quad (7)$$

Note that consistency requires a common zero-point (cf. an A0V star where $(V - R) = (V - K) = 0$).

We used previously published VRK photometry of η Aql (Barnes et al. 1997) to derive its apparent magnitude in the above bands as a function of phase by fitting a low-order Fourier series to the published photometry, after first correcting for the effects of reddening following the procedure outlined in Evans & Jiang (1993). The individual values of $E(B - V)$ were taken from Fernie (1990), and the reddening corrections applied are listed in Table 7. For each diameter measurement we then used the Fourier series to derive m_V and $V - K$ at the epoch of observation, and using Eq. 5 we derived the corresponding surface brightness. Results are shown in Figure 2 and listed in Table 8. We also performed this type of fit using ζ Gem data. In this case we used photometry from Wisniewski & Johnson (1968) and Moffett & Barnes (1984).

In Table 8 we compare the derived surface brightness relations to similar relations from work based on non-variable supergiants (Fouque & Gieren 1997) and other Cepheid observations (Nordgren et al. 2001). The F_V vs. $V - R$ fits can also be compared with the Gieren (1988) result that the slope of the $V - R$ surface brightness relation (c) is weakly dependent on pulsational period (P) according to

$$c = -0.359 - 0.020 \log P \quad (8)$$

which for η Aql predicts $c = -0.376$ and for ζ Gem $c = -0.379$. These comparisons reveal generally good agreement between the various relations in Table 8.

3.6. Period-Radius Relations

The relation between pulsational period and Cepheid radius has received considerable attention in the literature, primarily because early results based on different techniques were discrepant (Ferne 1984; Moffett & Barnes 1987). Period-radius relations are also useful in that they can indicate pulsation mode. This is important for calibrating period-luminosity relations since different modes will yield different relations (Feast & Catchpole 1997; Nordgren et al. 2001).

In Fig. 3 we compare our measured Cepheid diameters to the values predicted from a range of techniques: Bono, Caputo, & Marconi (1998) calculate a period-radius relation from full-amplitude, nonlinear, convective models for a range of metallicities and stellar masses. Gieren, Moffett, & Barnes (1999) use the surface brightness technique based on V and $V - R$ photometry and the Fouque & Gieren (1997) result to derive radii for 116 Cepheids in the Galaxy and the Magellanic Clouds. They find an intrinsic width in their relation of ± 0.03 in $\log R$. Laney & Stobie (1995) also use the surface brightness technique for estimating Cepheid diameters. However, they find that infrared photometry (K , $J - K$) is less sensitive to the effects of gravity and microturbulence (and presumably also reddening), and hence

Cepheid	A_V	A_R	A_K
η Aql	0.515	0.377	0.055
ζ Gem	0.062	0.046	0.007

Table 7: Reddening values used in deriving surface brightness parameters for η Aql and ζ Gem, based on values of $E(B - V)$ from Ferne (1990).

yields more accurate results. For shorter periods (≤ 11.8 days) their results indicate smaller diameters as compared to other relations.

Given the limited sample of only two radius measurements we can draw only preliminary conclusions: (1) the general agreement between our observations and the relations is good, and (2) the data seem to prefer a shallower slope than e.g. the Laney & Stobie (1995) relation. This latter observation will have to be confirmed with observations of shorter-period Cepheids.

4. Summary

We have measured the changes in angular diameter of two Cepheids, η Aql and ζ Gem, using PTI. When combined with previously published radial velocity data we can derive the distance and mean diameter to the Cepheids. We find η Aql to be at a distance of 320 ± 32 pc with a mean radius of $61.8 \pm 7.6 R_{\odot}$. We find ζ Gem to be at a distance of 362 ± 38 pc, with a mean radius of $66.7 \pm 7.2 R_{\odot}$, in good agreement with previous work. The precision achieved is $\sim 10\%$ in the parameters; further improvement is at present limited by our understanding of the details of the Cepheid atmospheres. In particular the details of limb darkening and projection factors need to be understood, with the projection factors being the largest source of systematic uncertainty.

We note that these results do not rely on photometric surface brightness relations, hence results derived here can be used to calibrate such relations. We performed such calibrations and found good agreement with previous results. We also note that at present we have derived distances to only two Cepheids, and although the derived distances are consistent with currently used period-luminosity relations, it will be necessary to observe several more Cepheids with this technique before worthwhile quantitative comparisons can be made.

Source	a	b	c
η Aql, this work	3.941 ± 0.005	-0.125 ± 0.004	-0.375 ± 0.002
ζ Gem, this work	3.946 ± 0.011	-0.130 ± 0.002	-0.378 ± 0.003
Fouque & Gieren (1997)	3.947 ± 0.003	-0.131 ± 0.003	-0.380 ± 0.003
Nordgren et al. (2000)	3.941 ± 0.004	-0.125 ± 0.003	-0.368 ± 0.007

Table 8: A comparison between the various surface brightness relations (see text for definitions).

In the near future long-baseline interferometers will provide a great deal of useful data in this area: in addition to further observations of the brightest galactic Cepheids, the very long baselines currently being commissioned at the Navy Prototype Optical Interferometer (Armstrong et al. 2001b) and the Center for High Angular Resolution Astronomy array (ten Brummelaar et al. 2001) will allow direct measurements of the limb darkening effects through observations of fringe visibilities past the first visibility null. Given the close relation between limb darkening and projection factors we expect that improvements in understanding one will improve our understanding of the other. It is also clear that additional photometry and radial velocity measurements would be very useful. In particular ζ Gem suffers from a lack of good infrared photometry, while concerns about level effects make infrared radial velocity measurements like those of Sasselov & Lester (1990) very desirable.

We thank D. Sasselov, A. F. Boden, M. M. Colavita, S. R. Kulkarni, and R.R. Thompson for valuable comments. We also wish to thank K. Rykoski for his excellent observational work. Observations with PTI are only made possible through the efforts of the PTI collaboration, for which we are grateful. Funding for the development of PTI was provided by NASA under its TOPS (Toward Other Planetary Systems) and ASEPS (Astronomical Studies of Extrasolar Planetary Systems) programs, and from the JPL Director’s Discretionary Fund. Ongoing funding has been provided by NASA through its Origins Program and from the JPL Directors Research and Development Fund. This work has made use of software produced by the Interferometry Science Center at the California Institute of Technology. This research has made use of the SIMBAD database, operated at CDS, Strasbourg, France. B.F.L gratefully acknowledges the support of NASA through the Michelson fellowship program.

REFERENCES

- Armstrong, J. T., Nordgren, T. E., Germain, M. E., Hajian, A. R., Hindsley, R. B., Hummel, C. A., Mozurkewich, D., & Thessin, R. N. 2001, *AJ*, 121, 476
- Armstrong, J. T. et al. 2001, American Astronomical Society Meeting, 198, 6303
- Albrow, M. D., Cottrell, P. L., 1994, *MNRAS*, 267, 548–556
- Barnes, T. G. & Evans, D. S. 1976, *MNRAS*, 174, 489.
- Barnes, T. G., Fernley, J. A., Frueh, M. L., Navas, J.G., Moffett, T. J., Skillen, I., 1997, *PASP*, 109,645–658.
- Bersier, D., Burki, G., Mayor, M., Duquennoy, A., 1994, *A&A*, 108, 25–39

- Bersier, D., submitted to ApJ.
- Bersier, D., Burki, G., Kurucz, R. L., 1997, A&A, 320, 228–236
- Boden, A. F., van Belle, G. T., Colavita, M. M., Dumont, P. J., Gubler, J., Koresko, C. D., Kulkarni, S. R., Lane, B. F., Mobley, D. W., Shao, M., Wallace, J. K., 1998, ApJ, 505, L39
- Bohm-Vitense, E. & Proffitt, C. 1985, ApJ, 296, 175–184.
- Bono, G., Caputo, F., & Marconi, M. 1998, ApJ, 497, L43
- ten Brummelaar, T. A. et al. 2001, American Astronomical Society Meeting, 198, 6106
- Claret, A., Diaz-Cordoves, J., Gimenez, A., 1994, A&ASS, 114, 247–252.
- Cohen, M., Walker, R., Carter, B., Hammersley, P, Kidger, M., Noguchi, K., 1999, AJ, 117, 1864–1889.
- Colavita, M. M., Wallace, J. K., Hines, B. E., Gursel, Y., Malbet, F., Palmer, D. L., Pan, X. P., Shao, M. , Yu, J. W., Boden, A. F., Dumont, P. J., Gubler, J. Koresko, C. D., Kulkarni, S. R., Lane, B. F., Mobley, D. W., van Belle, G. T, 1999, ApJ, 510 , 505–521.
- Colavita, M. M., 1999, PASP, 111, 111–117.
- ESA, 1997, The Hipparcos catalogue, SP-1200
- Evans, N. R., Jiang, J. H., 1993, AJ, 106, 726–733.
- Feast, M. 1999, PASP, 111, 775
- Feast, M. W. & Catchpole, R. M. 1997, MNRAS, 286, L1
- Fernie, J. D. 1984, ApJ, 282, 641
- Fernie, J. D., 1990, ApJS, 72, 153–162.
- Fernley, J. A., Skillen, I., & Jameson, R. F. 1989, MNRAS, 237, 947
- Fouque, P., Gieren, W.P., 1997, A&A, 320, 799–810.
- Gieren, W. P. 1988, ApJ, 329, 790.
- Gieren, W. P., Moffett, T. J., & Barnes, T. G. 1999, ApJ, 512, 553

- Hindsley, R., Bell, R. A., 1986, *PASP*, 98, 881–888
- Jacobsen, T.S., Wallerstein, G., 1981, *PASP*, 93, 481–485.
- Jacobsen, T.S., Wallerstein, G., 1987, *PASP*, 99, 138–140.
- Jacoby, G. H. et al. 1992, *PASP*, 104, 599
- Kervella, P., Coudé du Foresto, V., Perrin, G., Schöller, M., Traub, W. A., & Lacasse, M. G. 2001, *A&A*, 367, 876
- Krockenberger, M., Sasselov, D. D., & Noyes, R. W. 1997, *ApJ*, 479, 875
- Lane, B. F., Kuchner, M. J., Boden, A. F., Creech-Eakman, M., Kulkarni, R. R., 2000, *Nature*, 407, 485–487.
- Laney, C.D., Stobie, R.S., 1995, *MNRAS*, 274, 337–360
- Moffett, T. J. & Barnes, T. G. 1984, *ApJS*, 55, 389–432.
- Moffett, T. J. & Barnes, T. J. 1987, *ApJ*, 323, 280
- Nordgren, T., Armstrong, J.T., Germain, M.E., Hindsley, R.B., Haijan, A.R., Sudol, J.J., Hummel, C.A., 2000, *ApJ*, 543, 972–978.
- Nordgren, T., Lane, B. F., Hindsley R. B., submitted to *AJ*.
- Press, W.H., Flannery, B.P., Teukolsky, S.A., Vetterling, W.T., 1986, *Numerical Recipes* (New York: Cambridge Univ. Press).
- Ripepi, V., Barone, F., Milano, L., Russo, G., 1997, *A&A*, 318, 797–804
- Sabbey, C.N., Sasselov, D.D., Fieldus, M.S., Lester, J.B., Venn, K.A., Butler, R.P., 1995, *ApJ*, 446, 250–260
- Sasselov, D. D., Lester, J. B., 1990, *ApJ*, 362, 333–345.
- Szabados, L., 1991, *Comm. Konkoly Obs.*, No. 96.
- Tanvir, N. R. 1999, *ASSL Vol. 237: Post-Hipparcos cosmic candles*, 17
- Welch, D. L., 1994, *AJ*, 108, 1421–1426
- Wesselink, A. J., 1946, *BAN*, 368, 91

Wisniewski, W. Z., & Johnson, H. L. 1968, *Communications of the Lunar and Planetary Laboratory*, 7, 57

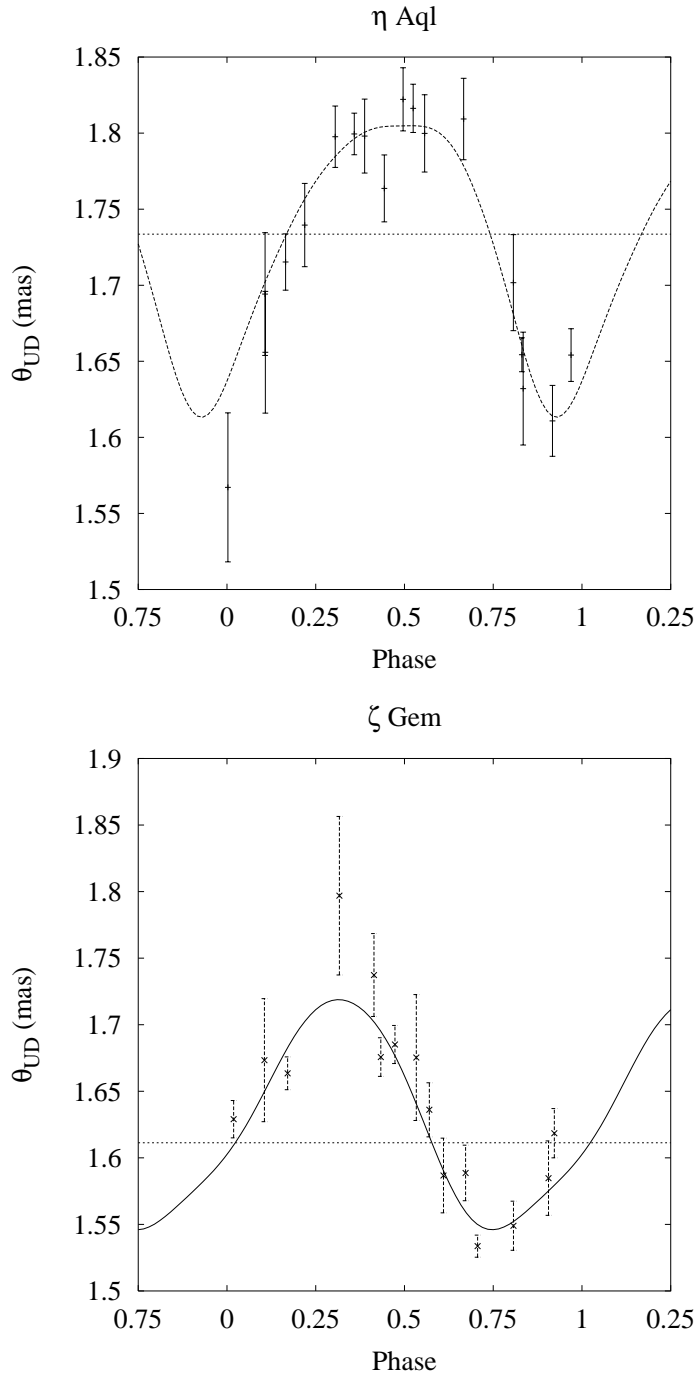


Fig. 1.— The angular diameters of η Aql (top) and ζ Gem (bottom) as a function of pulsational phase, together with a model based on radial velocity data, but fitting for distance, mean radius and phase shift. Also shown is the result of fitting a line to all the data. The fits are extended past phase 0 for clarity.

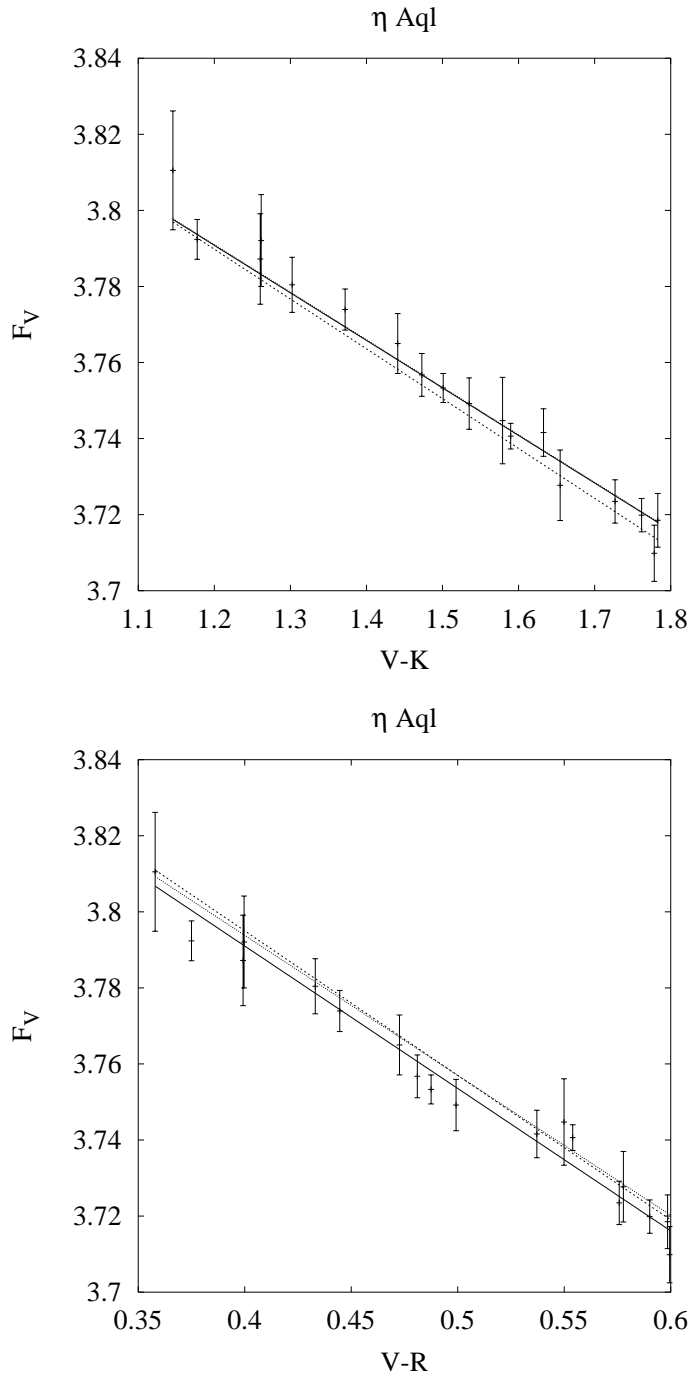


Fig. 2.— Dereddened F_V vs. $V - K$ (top) and $V - R$ (bottom) for η Aql. The solid line is the weighted linear least-squares fit to the data. The dashed line represents the relation from Fouque & Gieren (1997), and the dotted line represents the Nordgren et al. (2001) result.

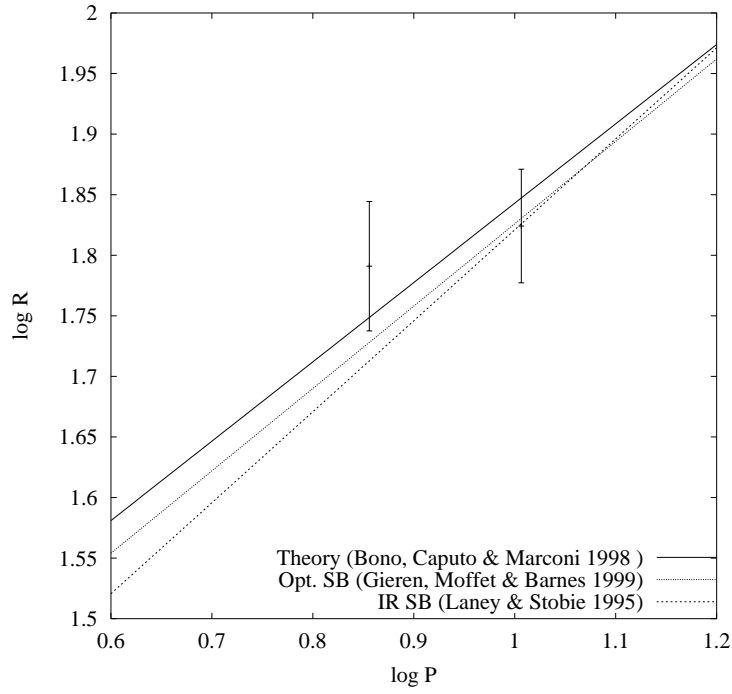


Fig. 3.— Period-radius diagram for the two Cepheids η Aql and ζ Gem, together with three relations available in the literature: a theoretical relation derived by Bono, Caputo, & Marconi (1998), an optical surface brightness relation from Gieren, Moffett, & Barnes (1999) and an IR surface brightness relation from Laney & Stobie (1995).